Ocean circulation at Axial Seamount in response to the 2015 eruption

Christine Bronder

University of Washington

School of Oceanography, Box 357940

Seattle, WA 98195-7940

bronderc@uw.edu

Abstract

Mid ocean ridges are large interruptions in the expansive abyssal plains that dominate ocean basins. Volcanically active ridges release heat and chemicals into the surrounding ocean through hydrothermal plumes. Benthic organisms are dependent on these plumes for nutrients and distribution of their larvae. Quantifiable changes in hydrothermal plumes have been documented in response to volcanic eruptions. These plumes experience increases in fluid temperature and rise height after eruptions and become event plumes. This study investigates the effects on circulation from the 2015 eruption at Axial Seamount: a submarine volcano located along the Juan de Fuca Ridge, 300 miles off the coast of Oregon. After the eruption, an unusual temperature increase was measured within the summit caldera. This increase is unique compared to other eruptions in that it is widespread, uniform, and has a large amplitude of 0.6 to 0.7 °C. Two hypotheses exist for the temperature anomaly: a large brine layer was expelled from the subsurface after the eruption, and a neutrally buoyant event plume formed above a lava flow and was advected above the summit. Since no salinity data is available, I evaluate the two hypotheses using the mean flow direction, magnitude, and variation of currents measured at a site within the caldera. There was an abnormal sustained flow to the southeast lasting 12 days with high speed coinciding with the rising temperature. This observation is consistent with the movement of a large volume of warm fluid. The increase in standard deviation and by proxy, turbulence, are not significant enough in the presence of increased flow speed to discriminate between a brine layer or event plume as the cause.

Plain Language Summary

Axial Seamount is an underwater volcano 300 miles off the coast of Oregon and recently erupted in 2015. Submarine volcanoes are important in supplying deep ocean environments with

heat and nutrients. I investigate the changes in circulation at the summit of the volcano after the eruption to understand what may have caused a large temperature increase that was observed at multiple locations at the summit. The temperature increase after the 2015 eruption differed from previous eruptions in that it was warmer and lasted longer. Analysis shows that large volume of fluid came from the northwest and moved through the south end of the caldera. Without salinity data available, the composition of this fluid could not be determined with confidence.

Introduction

Volcanically active mid-ocean ridges are large and important geologic features in ocean basins. They are responsible for the generation of new ocean crust on relatively short geologic time scales (Kelley et al, 2002). Basaltic melt from diverging plates creates new permeable ocean crust that allows seawater to circulate within it (Kelley et al, 2002). Circulating water within the crust is enriched in elements and heat which forms the foundation of benthic communities. Heated seawater reduces in density and rises buoyantly as a hydrothermal plume through vents scattered along the ridge. These hydrothermal plumes extend hundreds of meters into the surrounding ocean before becoming neutrally buoyant and being distributed by ocean currents releasing minerals and heat into the ocean (Lavelle and Mohn, 2010).

Mid ocean ridges present a large obstacle for the movement of bottom currents. Abyssal circulation is characterized by slow, cold, and dense currents running along the bottom of the ocean. Typically, ocean basins are large and flat with mixing occurring at the boundary layer of the seafloor (Drake et al, 2020). Mid ocean ridges rise 1000 – 2000 m above the seafloor and are rough in texture from faulting and solidified lava flows. The rough texture and increasing slope of these geologic features disturbs the flow and creates the potential for turbulent mixing.

An important implication of turbulent mixing and circulation across mid ocean ridges is the dispersal of biological larvae between vent systems (Lavelle and Mohn, 2010). Hydrothermal vents can be characterized as islands of life on the seafloor. They are home to rich and vibrant biological communities made of extremophiles that survive on chemosynthesis from dissolved minerals in expelled fluids by hydrothermal vents. These ecosystems are a relatively new discovery, and their dynamics are only beginning to become understood. Metaxas (2014) states that larval distribution is dependent on hydrodynamics as larvae are weak swimmers who must be passively disbursed around the environment. Understanding mixing and circulation around mid ocean ridges will further the understanding of how benthic organisms establish new communities.

Eruption events and their effects are rarely studied in situ as it is difficult to have measurement devices in place before an eruption. Observations are limited by the logistics of quickly planning research cruises after a confirmed eruption event (Xu et al, 2018). Axial Seamount, located on the Juan de Fuca spreading ridge off the coast of Oregon, has been a long studied volcanic site because of its relatively high activity. Eruptions occurred in 1998, 2011, and 2015 (Wilcock et al, 2018). Data has been collected over the span of three decades (Baker et al, 2019) with the most recent data coming from the Ocean Observatories Initiative (OOI) Regional Cabled Array. The Cabled Array, established in 2014, spans the region between Axial Seamount to the continental margin near Oregon. Funded by the National Science Foundation the Cabled Array aims to record 20 years of geologic, chemical, physical, and biological data to further the understanding of mid ocean ridge processes (Kelley et al, 2014). Of the three recent eruptions, the Cabled Array was in place for the 2015 eruption. It was able to collect data on the events preceding, during, and following the eruption. The eruption was preceded by inflation of

the caldera in the years before and high seismic activity starting when the sensors went online in November 2014 (Wilcock et al, 2018). Lava flows from this eruption were north of the caldera (Fig 1; Chadwick et al, 2016).

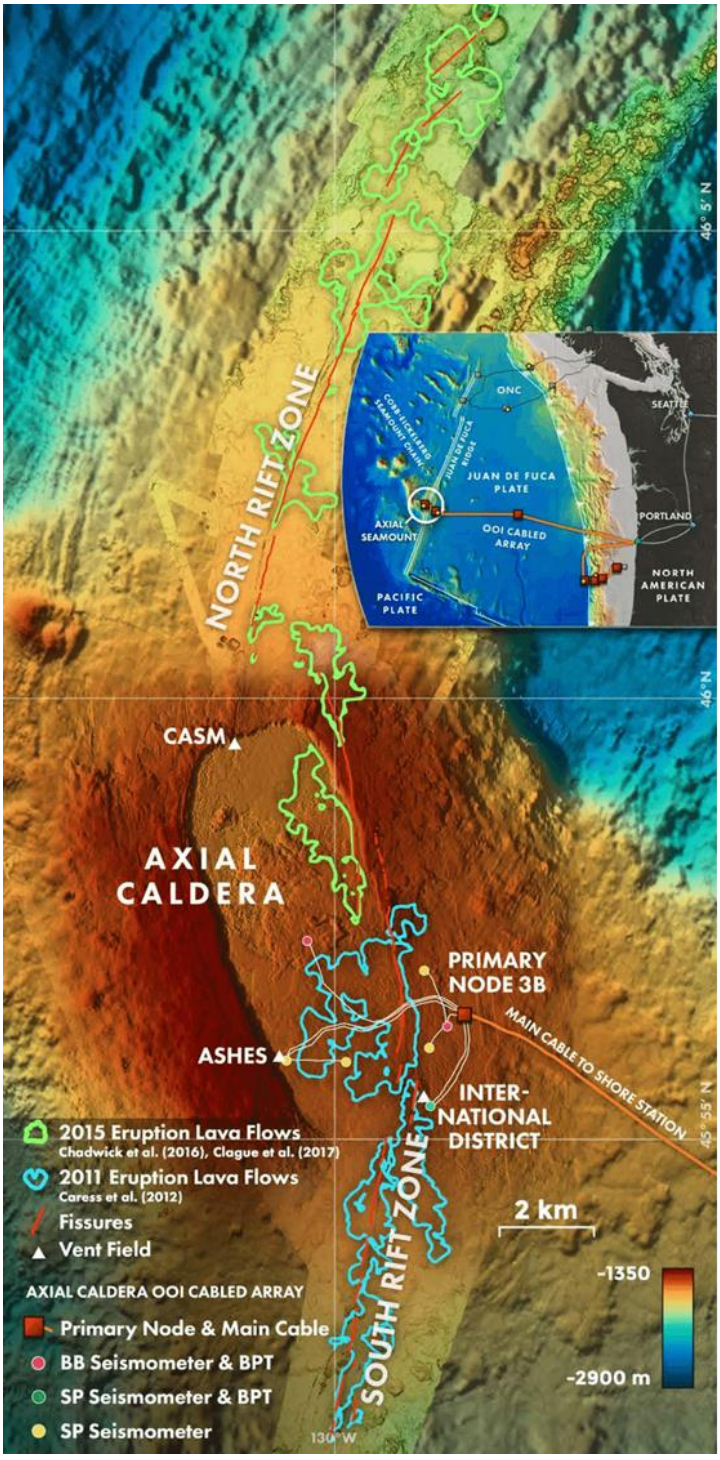

Figure 1. Detailed map showing the local bathymetry and location of Axial Seamount. The map identifies the location of lava flows of the 2015 eruption (green) and the fissures that run through the caldera and north rift zone. The International District is located at the southeast corner of the caldera where data for this study was collected (Wilcock et al, 2018).

Currents around Axial Seamount are essential in distributing heat, dissolved solutes, and organisms into the surrounding ocean. Currently, the most detailed information on circulation around the seamount comes from Xu and Lavelle's (2017) hydrodynamical model generated from current time-series data collected between 2001 and 2002. From the various generated velocity profiles, the model accurately predicts a cold dome of water around the top of Axial: a feature referred to as a Taylor's cap which is commonly found around seamounts (Lavelle and Mohn, 2010). Presence of the Taylor's cap helps to support the model's accuracy. The model also predicts a southward flow out of the caldera which is home to International District Vent Field. By comparing measured values gathered within the caldera by the Cabled Array, the predictive accuracy of the model can be verified.

Axial Seamount circulation is subject to perturbations caused by discharge of warm hydrothermal fluid. These eruptions increase the flux of hot fluids and materials leaving the vents, altering the chemistry of the water (Baker et al, 2019). These event plumes may result from the intrusion of magma causing a large release of hot water that was trapped in the crust (Lavelle and Mohn, 2010). Baker et al (2019) shows in their three decadal long study that hydrothermal plumes increase in rise height and turbidity lasting for years after eruptions. They demonstrate that the increased heat flow from dikes and lava flows increases the hydrothermal flow in each eruption. Considering the relationship between turbulence and velocity, an increase in velocity should cause an increase in turbulent mixing after the eruption.

In the days and weeks following the eruption in 2015, multiple sensors in the caldera recorded a seawater temperature increase of 0.6 to 0.7 °C. This is unusual compared to previous eruptions at Axial Seamount in which seawater increased from 0.2 to 0.5 °C over a shorter period of time (Xu et al, 2018). In previous eruptions the lava flows were within 100 to 600 m of the

sensors, while the 2015 eruption saw lava flows to the north, 1000 to 4000 m from the caldera (Xu et al, 2018). In order to account for the enduring temperature increase and the distance traveled to the caldera sensors, Xu et al (2018) proposed that a warm, dense, briny fluid was expelled from the subsurface after the eruption. The proposed brine layer would have a negative impact on the buoyant rise of hydrothermal discharge. If a decrease in turbulent mixing is observed in response to the eruption, this would imply an increase in stratification from the increased density of the discharged fluid.

The anomalous temperature increase in the caldera in the weeks following the eruption is currently only explained by the brine hypothesis. Event plumes can rise 1000 m into the surrounding ocean and are subject to mixing and diffusion. The temperature anomaly after the 2015 eruption was larger in amplitude than the temperature anomaly attributed to an event plume after the 1998 eruption (Baker et al, 2019). The data collected following the eruption is limited by the lack of salinity sensors within the caldera (Xu et al 2018). In the absence of salinity data, the brine hypothesis must be supported by indirect observations. The goal of this study is to test whether the observations after the 2015 eruption are consistent with the presence of a brine layer, by analyzing the changes in flow magnitude, variance, and direction. I hypothesize that there will be a decrease in turbulent mixing and circulation within the caldera of Axial Seamount after the eruption. The assumption that an inverse relationship exists between increased turbulent flow and the brine later will be used to interpret the results. A positive hypothesis will help support the brine hypothesis developed by Xu et al (2018) explaining the sudden and uniform increase in temperature at multiple sites around Axial Seamount after the eruption. It is possible that the opposite relationship exists and turbulent mixing increases from the increase in hydrothermal activity after eruptions demonstrated by Baker et al (2019). A third possible

scenario is that there is no significant relationship between flow variations and the temperature anomaly, and more investigation is required.

Methods

The OOI provides data free to the public for all of their sensor arrays worldwide. Data was acquired from their Data Portal: https://ooinet.oceanobservatories.org/. International District Vent Field 2 contains the only 3-d single point velocity meter in the caldera. The velocity meter is model VEL3DB class MAVS-4, and collects time-series velocity data in an (x,y,z) coordinate system as well as seawater temperature. It functions by sending out an acoustic signal and measuring the travel time of the signal to a receiver. Its velocity resolution is 0.3 cm s^{-1} and direction of ±2° with a sampling rate of 1 second for each component. Velocity and temperature data was acquired for the entire year of 2015. The hydrodynamic model of Axial Seamount was provided by its creator Guangyu Xu of the Applied Physics Laboratory, Seattle, WA. The model contained velocity time series at the International Vent District 2 between March 1, 2015 and June 30, 2015 (Guangyu Xu, personal communication).

The OOI data was masked to remove missing data and values outside of the ±17 cm s^{-1} range. These erroneous values were deemed excessive for the bottom 1 m where the velocity meter is located and are likely spurious. Values outside of this range were prevalent during the first few and last months of the year. Preliminary plots showed the temperature increase at the International District Vent Field 2 to occur between May 2 and May 25, 2015. To achieve a measure of variation, the velocity time series was resampled using standard deviation over 100 second intervals and then averaged over the course of a day for both the entire year and the eruption period of April 16 through May 25, 2015. Velocity over the course of the year and the eruption period without the resampling were averaged over the course of a day to analyze the

changes in flow direction. The root mean square was taken of the mean daily flows and added to a histogram to determine if flow is atypical post eruption. The northward and eastward flows were qualitatively compared to the northward and westward flows of Xu's model to verify its predictive accuracy.

Results

Figure 2 shows the current velocity and seawater temperature over the course of 2015 with the native sample rate of 1 second. Holes are present in the data where values larger than 17 cm s^{-1} were removed. The end of February and November through December experience large velocities in all three directions. These times periods had a large number of values that were removed when the dataset was initially masked to remove erroneous values. Northward velocity has spikes ranging between ±10 cm s^{-1}, eastward velocity: between ±7 cm s^{-1}, and upward: ranges between ±4 cm s^{-1}. Temperature experiences a several spikes throughout the year. Two of which occur during the same period that had multiple error values removed. Between May and June temperature increased from its usual 2.4 – 2.6 °C to over 3.2 °C.

Averaging the current velocities each day (Fig 3) leads to a smaller range than in Figure 2. Northward velocities range from ±2 cm s^{-1} but are primarily in the southward direction for most of the year. The eastward velocities range from -2 to 3 cm s^{-1}, but a primarily in the eastward direction. Upward velocities are small and typically don't exceed 0.2 cm s^{-1}. Temperature values have a smaller range as well, except for the large spike between April and May. Coinciding with the onset of this large temperature increase the flow is unidirectional with high speed to the southeast.

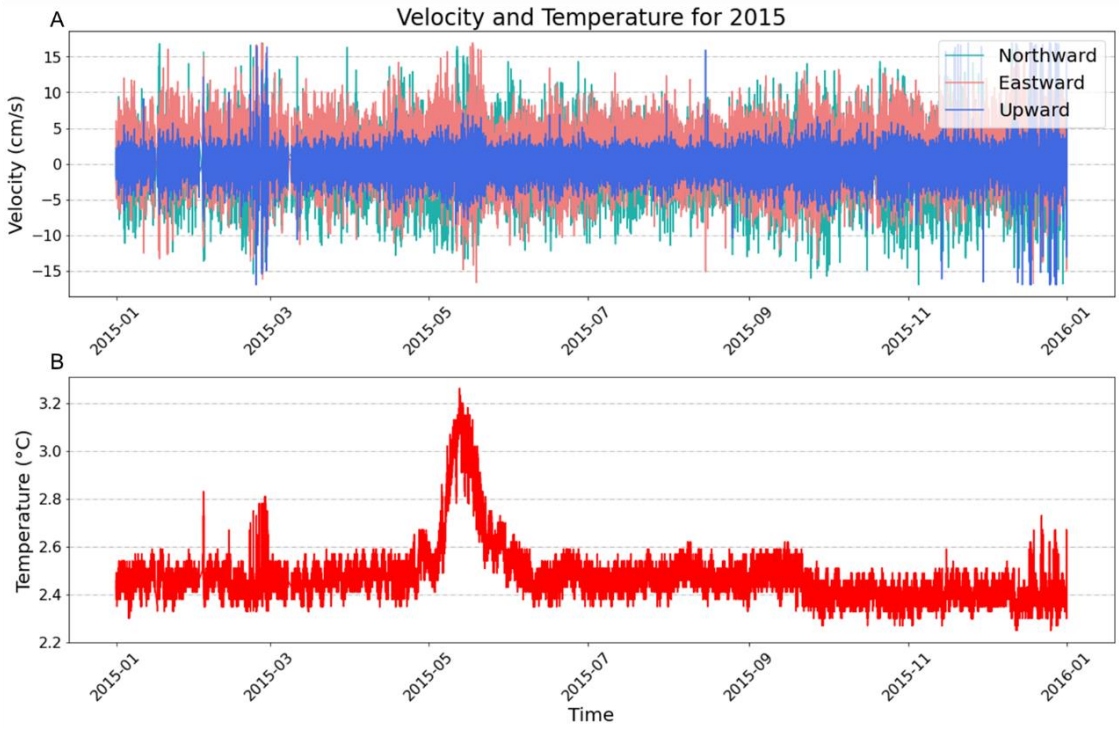

Figure 2. Current velocity at the International District Vent Field over the course of 2015 (A) compared to temperature (B).

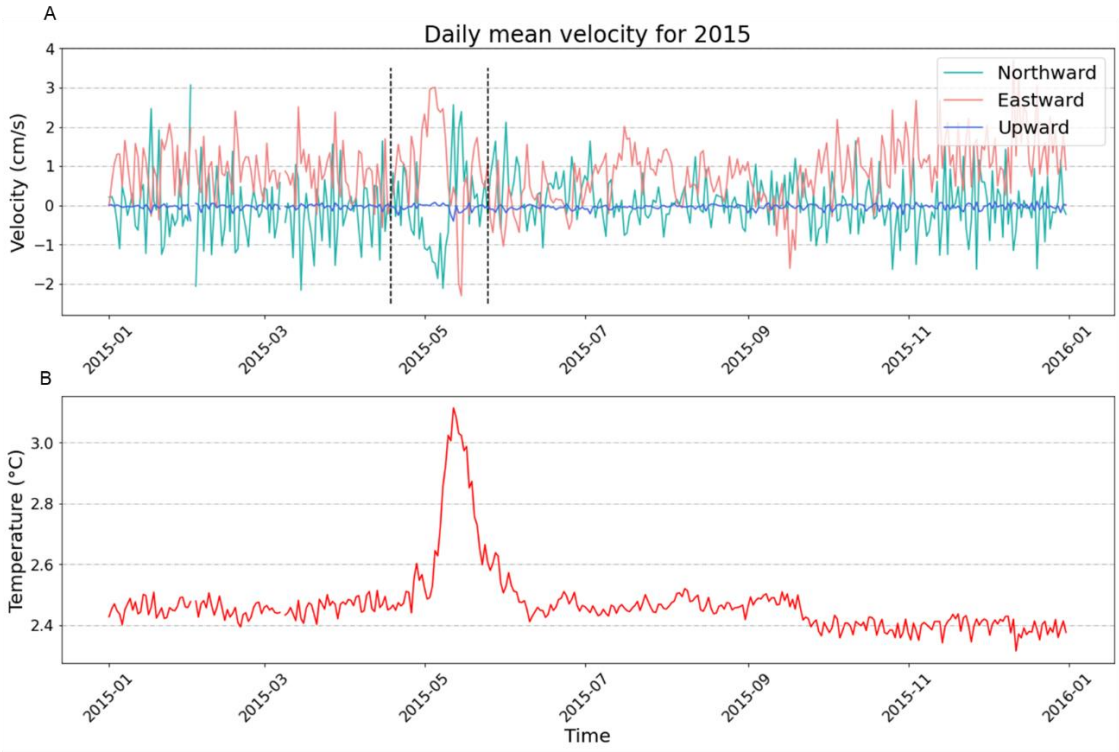

Figure 3. Daily mean flow for 2015 (A). Flow exhibits a general southeast trend .The dashed lines indicate the post-eruption period which noticeably displays a sustained flow that deviated from the pattern the rest of the year displays. Below is the daily mean time series for temperature (B).

This large, sustained flow at the International District Vent Field began 4 days after the eruption of Axial Seamount (Fig 4). There is a small increase in temperature a day after the eruption that subsides before temperature increases dramatically. The flow was constant in direction and fairly constant in magnitude until May 10, which is a day before the temperature reaches its maximum. At the maximum temperature and during the decrease, flow direction and magnitude vary in the horizontal planes. There is a slight downward flow at the maximum temperature point. Temperature returns to its normal range by May 24th, a month after the eruption of Axial Seamount.

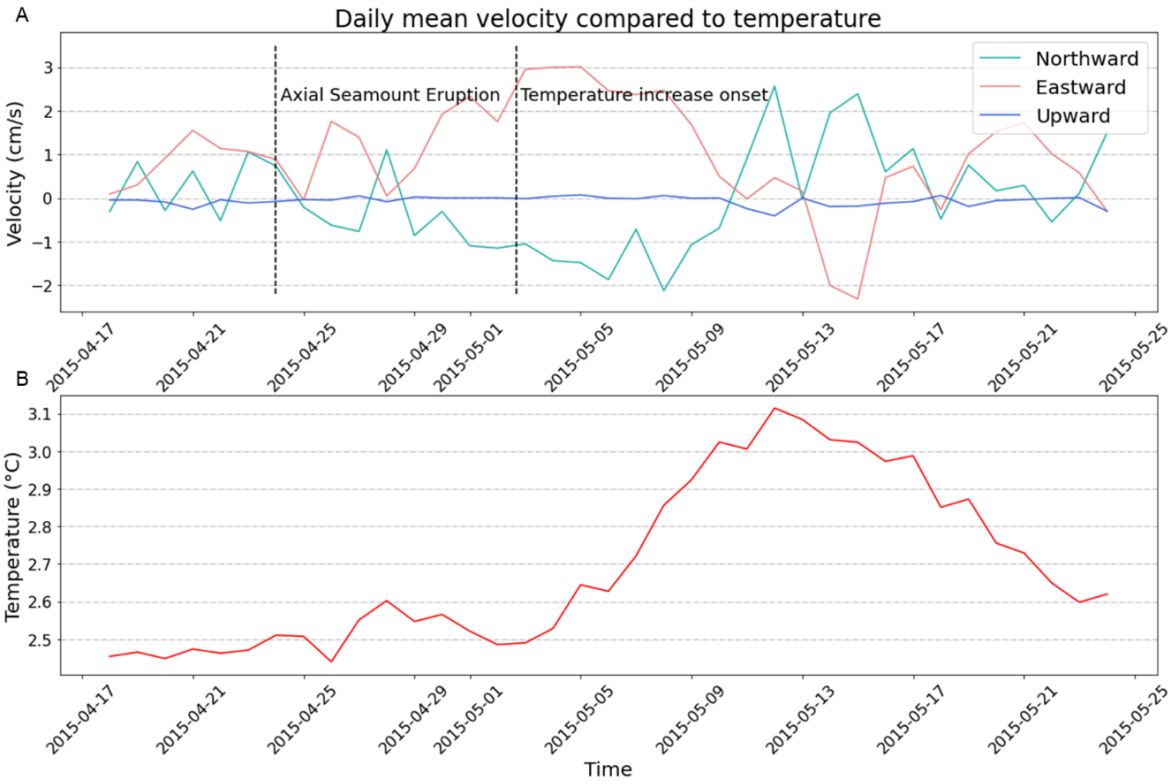

Figure 4. Daily mean flow for the post eruption study period (A). Notably, the sustained flow is only present when the temperature is actively increasing from April 28 through May 10 (B).

Figure 5 shows histograms of the root mean square velocities averaged over a day between the period of temperature increase, April 18 through May 25, and the rest of the year. The period of temperature increase, known as the excursion period henceforth, shows a wider

range and larger velocities occurring more often compared to the rest of the year. The northward and upward velocities over the year show almost an exponential decline in frequency with increasing magnitude. The excursion period encompasses 38 days, and the rest of the year is 327 days. The eastward velocity generally has larger magnitudes compared to the other two directions and the values are most frequent in the 0 to 1.7 cm s^{-1} range. Velocities greater than or equal to 2 cm s^{-1} in the eastward direction occur 20 times outside of the excursion period, accounting for 6.1% of the days. The excursion period has 8 occurrences of velocities greater than or equal to 2 cm s^{-1}, accounting for 21% of the days.

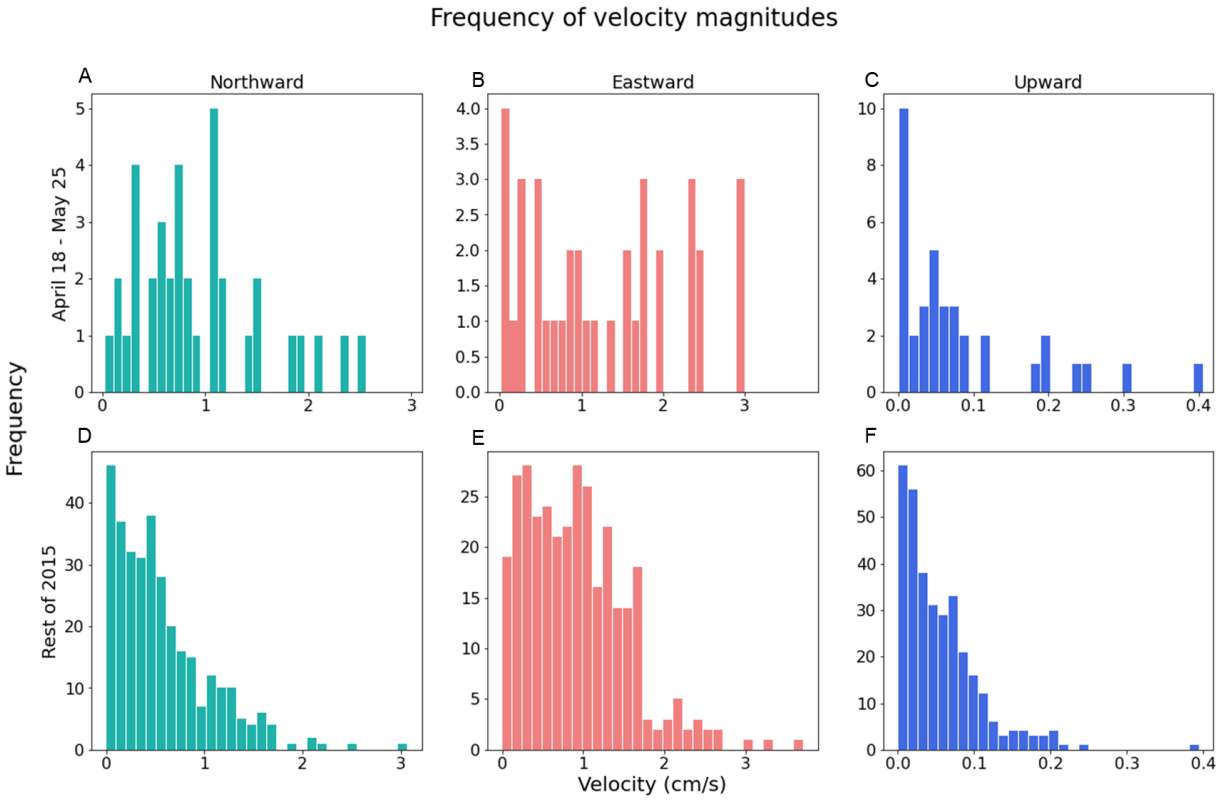

Figure 5. Frequency of root mean square velocities for the post eruption period (A, B, C) and the rest of the year (D, E, F). Larger velocities are more common during the post-eruption period and the rest of the year sees a logarithmic decline in frequency with increased magnitude. The number of samples for the post-eruption period is 38 days and the rest of the year composes 327 days.

The short-term standard deviation shows that all three velocities follow a similar trend in deviation from their respective means. Generally, all directions will either decrease or increase for a given day. Most of the year standard deviation stays within the range of 0.3 and 0.8 cm s^{-1}. The standard deviation has a few spikes throughout the year: beginning of February, April through May, and December. The February and December spikes occur where a large amount of erroneous values were removed from the data. The April through May spike in standard deviation occurs during the excursion period.

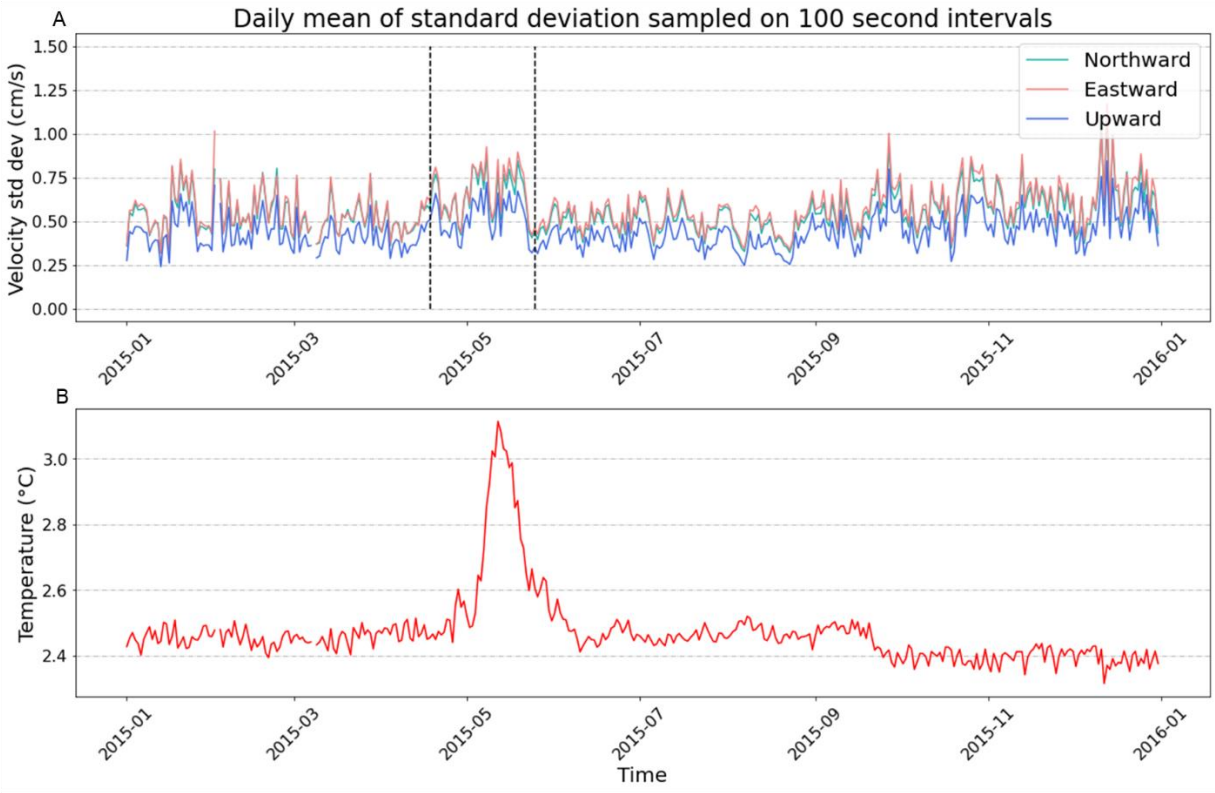

Figure 6. Time series of the standard deviation of flow over 100 s intervals averaged over a daily period for 2015 (A). Dashed lines indicate the post-eruption period and coincides with the 0.7 °C temperature increase seen in (B).

The standard deviation of velocity during the excursion period shows a slight increase during the duration of the temperature increase, with values decreasing during the maximum temperature. Values increase from ~0.5 cm s^{-1} to ~0.7 cm s^{-1} between the time before and during

the temperature increase. The standard deviations of the northward and eastward velocities are similar for the entire period while that for the upward velocity is generally 0.2 cm s^{-1} less than the other components.

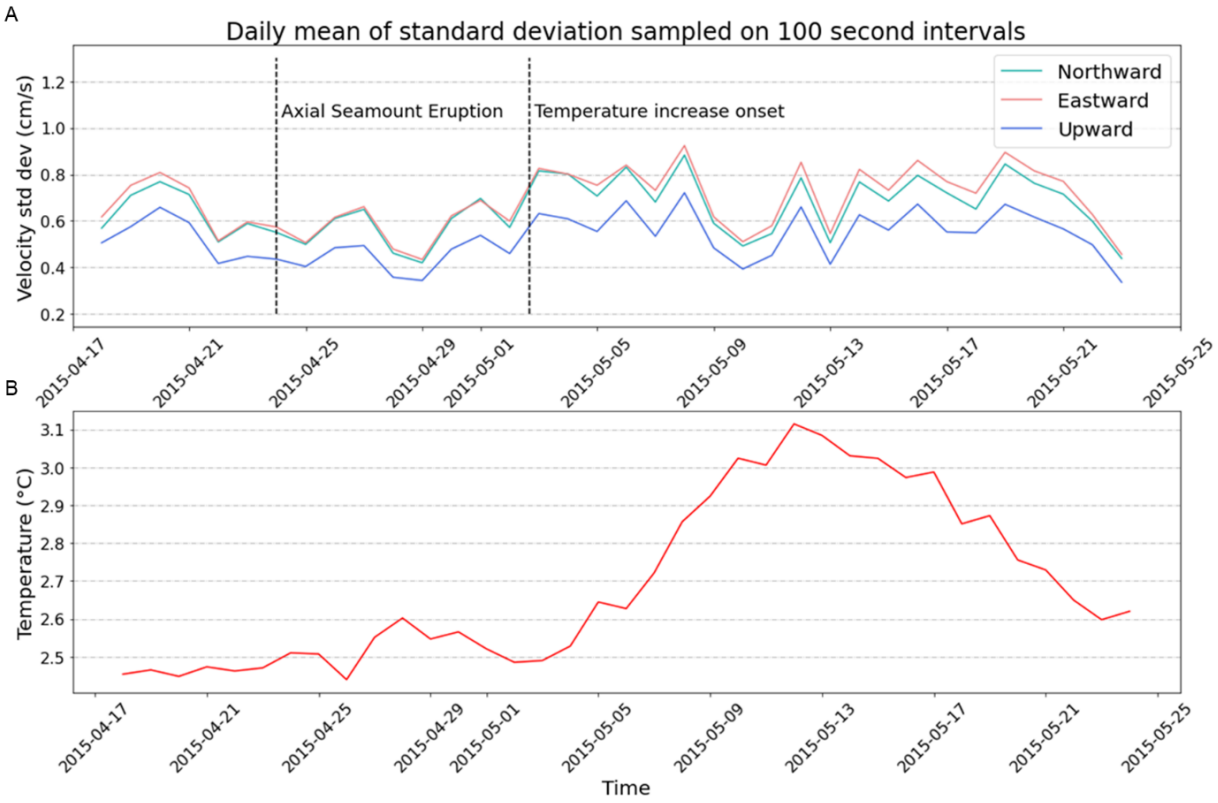

Figure 7. Time series of the standard deviation of flow over 100 s intervals averaged over a daily period between April 17, 2015 and May 25, 2015 (A). Deviation from the mean appears to increase sharply, to a maximum of 0.9 cm s^{-1} at the onset of the 0.7 °C temperature increase (B).

Figure 8 shows the frequency of daily averaged standard deviation between the excursion period and the rest of the year. The year shows a wider range in values and most of the values fall between the 0.3 and 0.6 cm s^{-1} range, with a few values of greater than 0.8 cm s^{-1}. The excursion period has a range of standard deviation values falling within the 0.4 to 0.9 cm s^{-1} range for northward and eastward velocities and 0.3 to 0.7 cm s^{-1} for upward velocity. The ranges of standard deviation between the excursion period and the rest of the year differ by 0.1 to 0.2 cm s^{-1}.

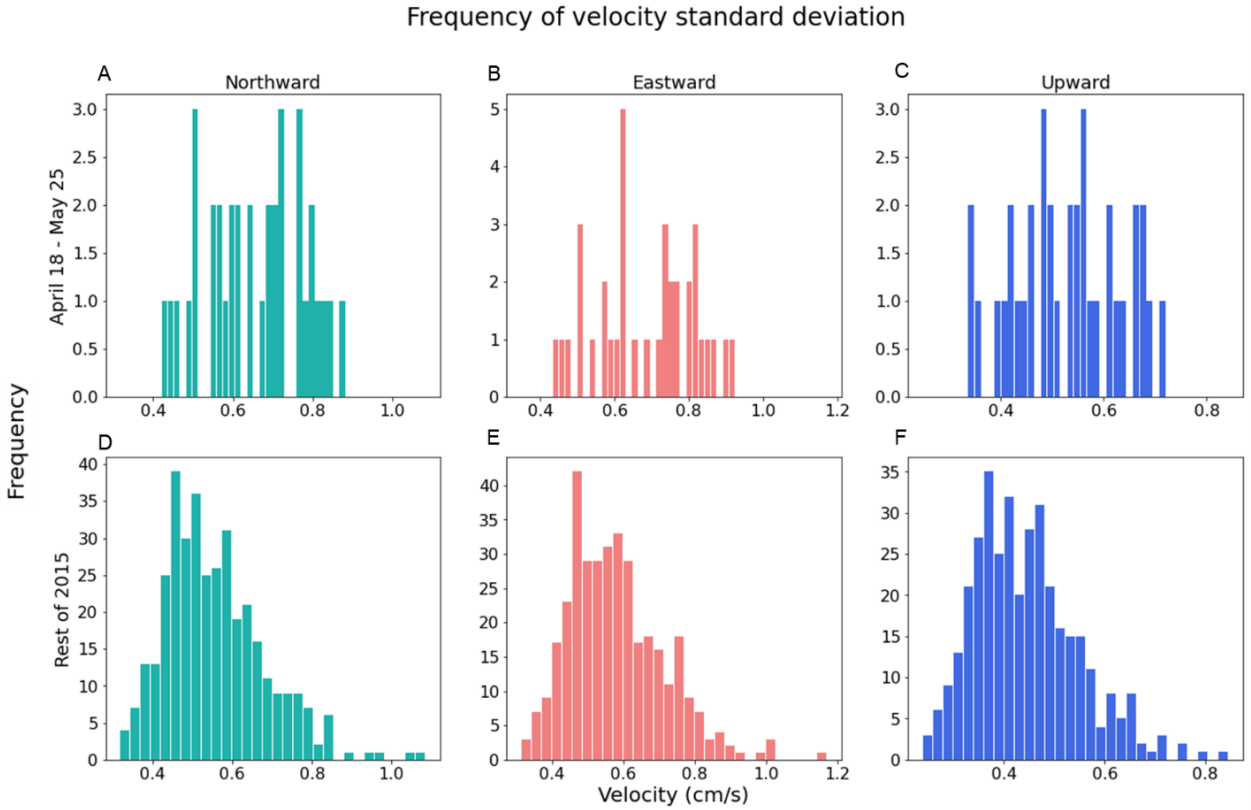

Figure 8. Frequency of daily averaged standard deviation values for velocity for the post eruption period (A, B, C) and the rest of the year (D, E, F). Standard deviation typically ranges from 0.3 to 0.6 for the majority of the year. The number of samples for the post-eruption period is 38 days and the rest of the year composes 327 days.

Velocities in the horizontal plane measured at Axial Seamount between March 1st and June 30th typically range from ±5 cm s^{-1} and are in the southeast direction (Fig 9). Values from the hydrodynamic model for the same period predict a large range in values, -30 to 20 cm s^{-1}, and changing direction of current flow. The model predicts that flow will be in the southeast direction for the first part of March, decrease to zero around April, be in the northwest direction in the beginning of May, southwest at the end of May and northwest for the month of June. The measured velocity does not experience any sustained changes in flow direction that the model predicts but stays in the same direction with small changes in direction happening on the scale of hours to days.

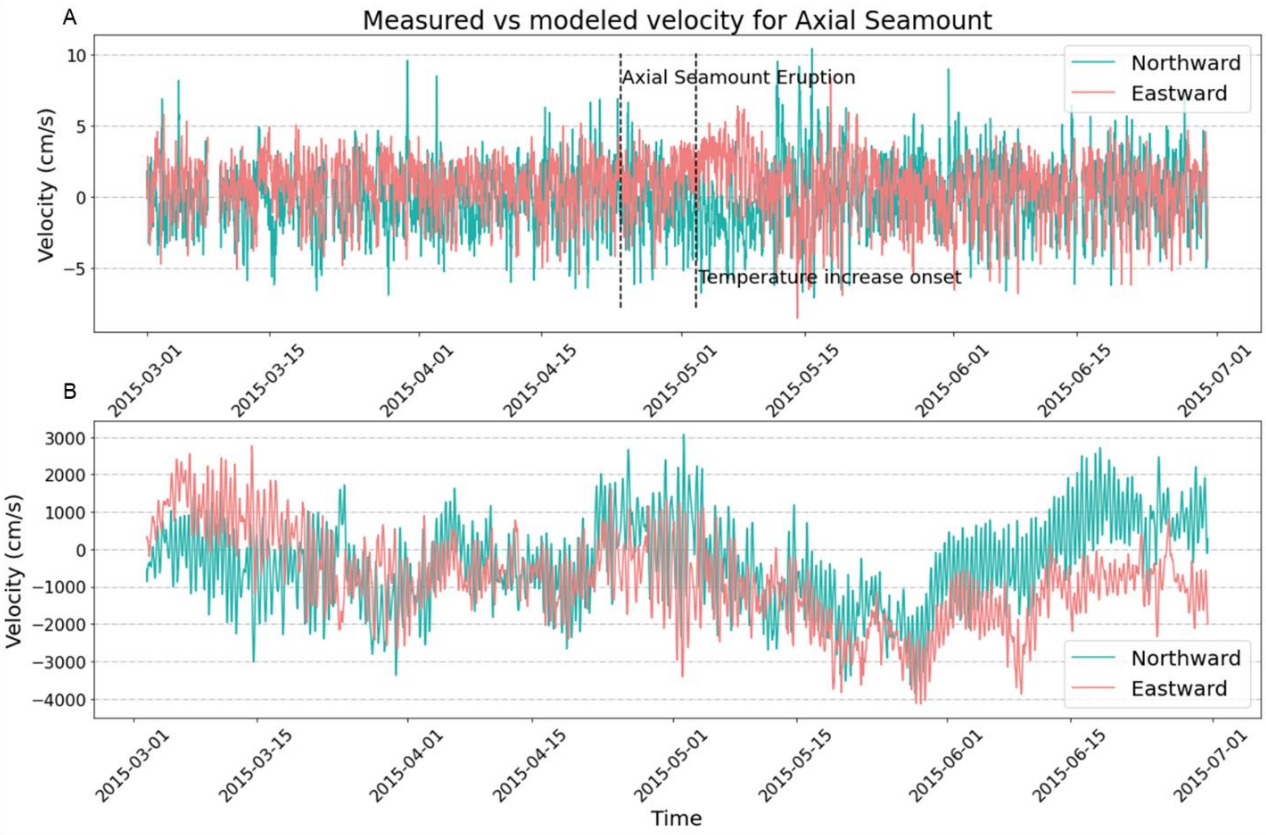

Figure 9. Half-hourly mean velocity in the northward and eastward direction measured from the Regional Cabled Array (A) compared to the predicted mean velocity from the hydrodynamic model of Axial Seamount (B). The model measures velocity over the bottom 10 m resulting in larger magnitudes compared to the collected data.

Discussion

The temperature anomaly seen in April and May (Fig 2) is striking and significant given that temperature typically ranges from 2.4 to 2.6 °C in 2015. The amplitude of the peak is an order of magnitude larger than other peaks from normal seawater temperature. The sustained flow as seen in Figure 3 is highly abnormal and unusual compared to the velocities for the rest of the year (Fig 5). The only other time at which velocities reach this high speed is at the end of February and at the end of the year. The high velocities experienced at the end of February and at the end of the year (Fig 2) are possibly corrupted by bad data. February and the end of the year had many clusters of velocity values ranging from 25 to 200 cm s-1 and missing data. The

large values that are left over likely don't correspond to any real event. The excursion period did not experience the same clustering of exceptionally large values, so the data from this period can be considered valid.

The persistent flow shows that a large amount of warm fluid moved through the International District Vent Field from the northwest direction (Fig 3; Fig 4). The flow could be explained by either of two hypotheses. It is possible that a large brine layer was expelled in the north of the caldera and flooded the vent field as it flowed out of the south end of the caldera. It is also possible that an event plume with normal anticyclonic flow (Lupton et al, 1998) moved into the vent field post eruption. A brine layer would require a very large amount of fluid in order to be consistent with the observations at the other vent fields (Xu et al, 2018). An event plume would be large enough to cover multiple sites within the caldera; however, event plumes usually have temperature anomalies <0.2 °C (Baker et al, 2019) which is much smaller than the observed temperature increase. The flow direction to the southeast observed during the excursion period is inconsistent with where the event plume would originate over the northern lava flows. The event plume from the north would show flow to the southwest during the initial temperature increase as it moved southward from the lava flows.

Since no salinity data is available for 2015, the standard deviation of flow serves as a proxy for turbulence. I assume that turbulence is dependent on the density of the fluid and the possible increase in stratification that would occur in the presence of this brine layer. The standard deviation likely has the same errors in February and at the end of the year as the averaged velocity does (Fig 6; Fig 8). The standard deviation sees an increase during the temperature increase (Fig 7), and it is difficult to say whether or not turbulence is changed by the composition of the fluid. The increased standard deviation is likely a result of the increased

magnitude of flow during that same time period (Fig 4). Increased magnitude of flow over a rough surface could have been enough to increase the potential of turbulent mixing even in the presence of the hypothesized dense brine layer that would increase stratification. The increase in standard deviation is not definitive enough to rule out the presence of the brine layer or confirm its absence.

The model supplied by Guangyu Xu is an updated version of the one used to predict the movement of the brine layer in Xu et al (2018). Comparing the model to the velocity measurements from the Regional Cabled Array (Fig 9) shows that there is very little in common. The largest difference is in the scale of the velocities. The model predicts the flow averaged over the bottom 10 m at the International District. Velocities typically decrease logarithmically when they approach a boundary due to frictional forces. It is to be expected that the model generates velocities that are approximately 3 times larger than the velocities collected within a meter of the seafloor at the caldera. The direction of the model varies more over the 4-month period in which they were compared. It starts with flows typically in the southwest direction and ending with flows in the northwest direction, while the collected data stays generally in the southeast direction. This could be an effect from the different depth range between the datasets. Axial Seamount typically experiences anticyclonic circulation around the peak (Xu and Lavelle, 2017) and this could be affecting flow direction in the bottom 10 m of the model. The model was intended to show larger scale circulation than what was measured at one point in a vent field. Unless the values for one of the datasets can be confidently scaled, the model doesn't provide an accurate prediction of velocity at the International Vent District 2.

Conclusion

The sustained flow during the period of temperature increase strongly implies that a large amount of fluid was released as a result of the eruption. This kind of flow is not seen at any other point during the year. This suggests that circulation can be altered by volcanic eruptions. The flow direction during the temperature increase also suggests that the fluid is coming from the north of the International District, which is where the lava flows emerged during the 2015 eruption. The variations in standard deviation and by proxy, turbulence, are not significant enough to imply anything about the density of the fluid. It is possible that this large expulsion of fluid could be the result of a subsurface brine layer or an event plume. Without the availability of salinity measurements, it is difficult to predict the composition of this fluid and what that means about its source.

Acknowledgements

First and foremost, I want to express my thanks to my mentor, Professor William Wilcock for his patience, encouragement, and guidance during the process of creating, analyzing, and writing my senior research thesis. It was a fun and exciting experience to investigate data that had never been looked at before. Thank you for everything. My thanks also goes to Dr. Guangyu Xu for his valuable insight and the generosity of supplying me with his circulation model of Axial Seamount. I would like to thank the Ocean Observatories Initiative for collecting and hosting the data which made this study possible. Lastly, I would like to thank the 2021 senior thesis cohort for their support and comradery during these difficult times

References

Baker, E. T., S. L. Walker, W. W Chadwick Jr., D. A. Butterfield, N. J. Buck, and J. A. Resing. 2019. Posteruption enhancement of hydrothermal activity: A 33-year, multieruption time series at Axial Seamount (Juan de Fuca Ridge). Geochemistry, Geophysics, Geosystems, **20**:814-828.

Chadwick, W. W., J. B. Paduan, D. A. Clague, B. M. Dreyer, S. G. Merle, A. M. Bobbitt, D. W. Caress, B. T. Philip, D. S. Kelley, and S. L. Nooner. 2016. Voluminous eruption from a zoned magma body after an increase in supply rate at Axial Seamount. Geophysical Research Letters. **43**:12,063-12,070. doi:https://doi.org/10.1002/2016GL071327

Drake, H. F., R. Ferrari, and J. Callies. 2020. Abyssal Circulation Driven by Near-Boundary Mixing: Water Mass Transformations and Interior Stratification. Journal of Physical Oceanography. **50**:2203–2226.

Kelley, D., J. Baross, and J. Delaney. 2002. Volcanoes, fluids, and life at mid-ocean ridge spreading centers. Annual Review of Earth and Planetary Sciences. **9**:385–491.

Kelley, D., J. Delaney, and S. Juniper. 2014. Establishing a New Era of Submarine Volcanic Observatories: Cabling Axial Seamount and the Endeavour Segment of the Juan de Fuca Ridge. Marine Geology **352**. doi:10.1016/j.margeo.2014.03.010

Lavelle, J.W. and C. Mohn. 2010. Motion, Commotion, and Biophysical Connections at Deep Ocean Seamounts. Oceanography. **23**:90-103.

Lupton, J. E., E. T. Baker, N. Garfield, G. J. Massoth, R. A. Feely, J. P. Cowen, R. R. Greene, and T. A. Rago. 1998. Tracking the Evolution of a Hydrothermal Event Plume with a

RAFOS Neutrally Buoyant Drifter. Science **280**: 1052–1055. doi:10.1126/science.280.5366.1052

Metaxas, A. (2004). Spatial and temporal patterns in larval supply at hydrothermal vents in the northeast Pacific Ocean. Limnology and Oceanography. **49**:1949-1956.

Wilcock, W., R. Dziak, M. Tolstoy, W. Chadwick, and S. Nooner. 2018. The Recent Volcanic History of Axial Seamount: Geophysical Insights into Past Eruption Dynamics with an Eye Toward Enhanced Observations of Future Eruptions. Oceanography. **31**:114–123. doi:10.5670/oceanog.2018.117

Xu, G. and J.W. Lavelle. 2017. Circulation, hydrography, and transport over the summit of Axial Seamount, a deep volcano in the Northeast Pacific. Journal of Geophysical Research. **122**:5404–5422, DOI:10.1002/2016JC012464.

Xu, G., W.W. Chadwick, W.S.D. Wilcock, K.G. Bemis, and J. Delaney. 2018. Observation and Modeling of Hydrothermal Response to the 2015 Eruption at Axial Seamount, Northeast Pacific. Geochemistry, Geophysics, Geosystems. **19**:2780-2797. https://doi.org/10.1029/2018GC007607